X-ray-induced water vaporization

B. M. Weon,[1,*] J. S. Lee,[1] J. H. Je,[1,†] and K. Fezzaa[2]

[1]*X-ray Imaging Center, Department of Materials Science and Engineering, Pohang University of Science and Technology, San 31, Pohang 790-784, South Korea*

[2]*X-ray Science Division, Advanced Photon Source, Argonne National Laboratory, 9700 South Cass Avenue, Argonne, Illinois 60439, USA*

(Received 7 June 2011; published 26 September 2011)

We present quantitative evidence for x-ray-induced water vaporization: water is vaporized at a rate of 5.5 pL/s with the 1-Å-wavelength x-ray irradiation of ∼0.1 photons per Å^2; moreover, water vapor is reversibly condensed during pauses in irradiation. This result fundamentally suggests that photoionization induces vaporization. This phenomenon is attributed to surface-tension reduction by ionization and would be universally important in radiological and electrohydrodynamic situations.

DOI: 10.1103/PhysRevE.84.032601 PACS number(s): 68.03.Fg, 68.03.Cd, 87.59.−e, 78.70.−g

X-ray photonics is undergoing a revolution in imaging capabilities with the use of ultrabright x-ray sources. X-ray imaging at nano- and microscale is of great interest for applications in physical and life sciences, including x-ray physics, materials science, biological imaging, environmental analysis, archaeology, paleontology, and heritage restoration [1], because it facilitates the nondestructive, direct visualization of internal structures or elements. Meanwhile, radiation damage from the energy deposited into the sample by the x-ray photons used for imaging is inevitable [2,3]. In particular, radiation-induced ionization ultimately disintegrates the sample by charge accumulation beyond a limit and is otherwise known as Coulomb explosion [2,3] and fission [4,5]. The conventional damage barrier for Coulomb explosion is known to be about 200 photons per Å^2 for x rays with a wavelength of 1 Å [2,3]. Radiation damage can be mitigated by cryofixation or by ultrabright, ultrashort x-ray pulses [2]. However, radiation damage to living tissues by radiation ionization is not yet fully understood [6], although it is a limiting factor in achieving high-resolution data [2].

In previous works, we demonstrated that high-brilliance x-ray photons affect the surface tension of water by inducing ionization, using hard x-ray imaging at the 7B2 beamline (dose rate ∼1 kGy s^{-1}) of the Pohang Light Source [7–9]. A charge density over ∼10^{-4} charges per Å^2 was required for a significant reduction (>30%) in the surface tension [9]. This condition corresponds to x-ray irradiation of ∼0.1 photons per Å^2, following a simulation using the ionization rate of ∼1 charge per Å^2 by 2000 photons per Å^2 with x rays of 1 Å wavelength [2]. We put forward a possibility of water vaporization by surface-tension reduction [7,8] based on a monotonic relationship of the surface tension to the vaporization enthalpy [10,11], but quantitative evidence was lacking.

To corroborate the possibility, we conducted an elaborate experiment in a different synchrotron source while applying high-speed x-ray imaging [12,13]. Using a hydrophilic capillary tube containing a small amount of water, we first made a confined water lens with concave menisci, where the left region was *closed*, and the right one was *open* in air (Fig. 1). The changes of the water menisci were simultaneously imaged using a high-speed camera, synchronized and gated to the x-ray pulses. The image size was 768 × 640 pixels (0.98 μm per pixel, 16-bit). The field of view was larger than the capillary inner diameter ($2R = 500$ μm). Two repeatable shutter modes were used by (i) applying a short exposure for 100 ms (to see the radiation effect) and by (ii) taking a long recess for 9.9 s (to see any possible recovery) (Fig. 1). The undulator source at the XSD 32-ID beamline of the Advanced Photon Source of the Argonne National Laboratory provided the high x-ray brilliance necessary for the investigation of the x-ray-induced effects. The undulator gap was set to 31 mm, and most of the beam intensity was confined within the first harmonic at ∼13 keV (1 Å wavelength), with a peak irradiance of ∼10^{14} photons mm^{-2} s^{-1}/0.1% bw (equally ∼1 ph Å^{-2} s^{-1}/0.1% bw), as checked by the energy spectrum from the undulator. The x-ray photons were irradiated into the confined water by this high-brilliance white x-ray beam. At the sample location (∼37 m from the source), the beam profile [or the two-dimensional (2D) total intensity distribution for an on-axis aperture] showed that the capillary aperture was quasiuniformly illuminated since $2R$ was much smaller than the beam size. Here, the irradiation for the short exposure of 100 ms was ∼0.1 ph Å^{-2}. The exposure time for each frame was 1 ms, and 100 frames were taken in every short exposure of 100 ms, resulting in a single movie of 8000 frames during the total running time of 790.1 s.

We used a biconcave water plug within a hydrophilic capillary tube (Fig. 2), which mimics liquid plugs in pulmonary airways [14], for simplicity in the analysis of radiation effects. The water meniscus was always hemispherical within the tube and was not changed by x-ray irradiation. The x-ray-induced reduction in the surface tension changed the vaporization enthalpy and therefore the meniscus position. To monitor the meniscus position, we used high-speed phase-contrast x-ray imaging [12]. The x-ray wavelength of ∼1 Å from the brightest peak (∼0.1 ph Å^{-2}) corresponded to the dose rate of ∼50 kGy s^{-1}, which is higher than that for the previous works (∼1 kGy s^{-1}) [7].

Representative sequential images for a single cycle of x ray on-off switches are demonstrated in Fig. 2 for 10.001 s. The most obvious findings are the rightward gradual shifts in

*bmweon@hotmail.com
†jhje@postech.ac.kr

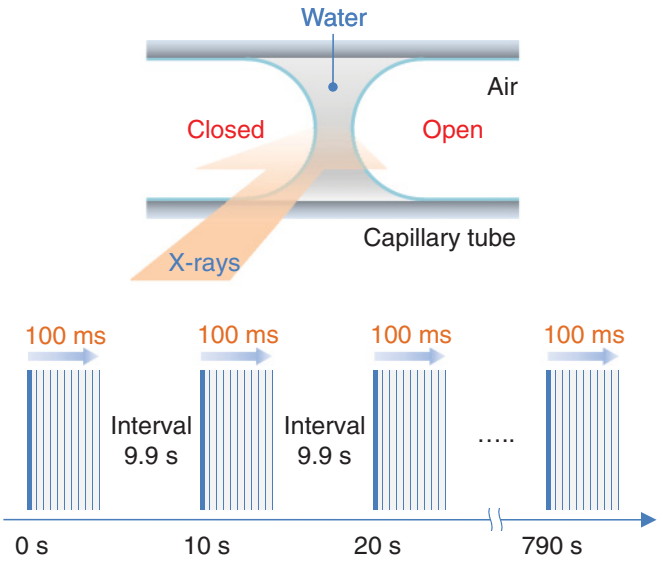

FIG. 1. (Color online) Schematic diagram of the experimental setup and the irradiation scheme. We used a confined water plug with biconcave menisci, where the left region was closed and the right one was open in air. A high-brilliance white x-ray beam achieved the irradiation and precise tracking of the menisci. Two different repeatable shutter modes were used by (i) applying a short exposure for 100 ms (for the radiation effect) and by (ii) taking a long pause for 9.9 s (for the possible recovery) in a single movie of 8000 frames for 790.1 s.

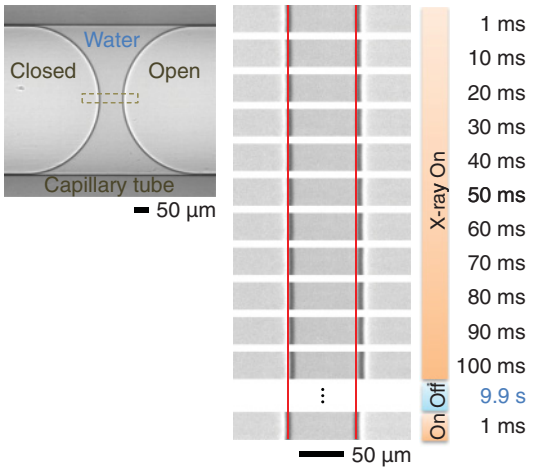

FIG. 2. (Color online) Sequential x-ray images for the first x-ray on-off cycle. Rightward gradual shifts appeared in both of the water menisci upon the short exposure of 100 ms. The original positions of the water menisci are marked by the solid lines. This image sequence clearly illustrates the expansion of the closed air volume because of the generation of water vapor by the irradiation at ~0.1 ph Å^{-2}. The left meniscus fully recovered to the initial position, whereas the right one did not, after the long 9.9 s pause of irradiation (see, in the image, 10 s and 1 ms). The leftward shift at the right meniscus shows the existence of natural vaporization into the atmosphere. The same behavior was repeated at every cycle of x-ray on-off switches.

both of the water menisci during the short exposure of 100 ms. The rightward shifts (~3.9 μm for 100 ms) clearly indicate the expansion of the closed air volume and thus represent the generation of water vapor by the irradiation. Interestingly, the shifts recovered upon the long 9.9 s pause of irradiation. Here, we note that the recovery behaviors were different between the left (closed) and right (open) menisci: the left one fully recovered to the initial position, whereas the right one did not. The right meniscus rather showed a slight leftward shift from the original position (~1.0 μm for 10 s). This shift clearly shows the existence of natural vaporization into the atmosphere. The leftward shift by natural vaporization was negligible during the short exposure of 100 ms, compared with the irradiation-induced rightward shift. This behavior [i.e., the recovery (leftward shift) of the left (right) meniscus after the long recess] was repeated for every cycle of x ray on-off switches (see, for instance, Supplemental Material for a sequential movie [15] for the first five cycles).

Figure 3 quantitatively shows the variance in the positions of the left (marked as X_L) and right meniscus apexes (marked as X_R) for the ten cycles of 100.1 s. The position changes during the irradiation of 100 ms and the pause of 9.9 s were very repeatable for every cycle. Here, the rapid shifts of 3.9 μm for 100 ms in both X_L and X_R were induced by the x-ray irradiation of ~0.1 ph Å^{-2}. After the 9.9 s pause, the left meniscus was completely recovered, as can be clearly seen by the same positions of the circles in Fig. 3(a). In contrast, the position of the right meniscus continued to decrease with time, as seen by the squares in Fig. 3(b). The gradual decreases in X_R at a rate of 1.0 μm for 10 s were induced by the natural vaporization. This result shows that the x-ray-induced switching is reversible in both of the menisci.

Now we discuss the x-ray-induced vaporization rate. As the volume change of water for the short exposure of 100 ms is not detectable, the vaporization rate was estimated from the water vapor expansion, measured as ~770 pL for 100 ms from the volume variance $\Delta V = \pi R^2 \Delta X_L$, where the meniscus radius $R = 250$ μm and the shift $\Delta X_L = 3.9$ μm for every cycle. This expansion is a direct result of the x-ray-induced effects. When water turns into water vapor, assuming the ideal gas law, the volume expansion is approximately 1400 times at 300 K. From the vapor expansion rate, 7.7 nL s^{-1}, and the volume expansion, 1400 times, we estimated the x-ray-induced vaporization rate as 5.5 pL s^{-1} by the irradiation of ~0.1 ph Å^{-2}. The large amount of water vapor generated at the closed region implies that x-ray-induced water vaporization might be a critical damaging factor of biological imaging.

The x-ray-induced vaporization rate at the closed region is quantitatively different with the natural vaporization rate at the open region. As demonstrated in Fig. 4, natural vaporization occurred only at the open (right) region, not at the closed (left) one. The natural water vaporization rate was estimated to be 20 ± 0.6 pL s^{-1} for the total cycles of 740 s at 20% humidity (Fig. 4), measured from the water volume changes based on the leftward shifts in X_R. Here the contribution of the x-ray-induced vaporization for each cycle was negligible, at ~0.5 pL (≈5.5 pL s^{-1} × 100 ms), compared with ~200 pL (≈20 pL s^{-1} × 10 s) by natural vaporization.

In comparison, the natural evaporation rate for a similar open-closed capillary system ($2R = 800$ μm) (Fig. 5) was separately measured as ~14 pL s^{-1} [=slope (6.4 × 10^{-5} s^{-1}) × initial volume (212 nL); half-closed circles] at

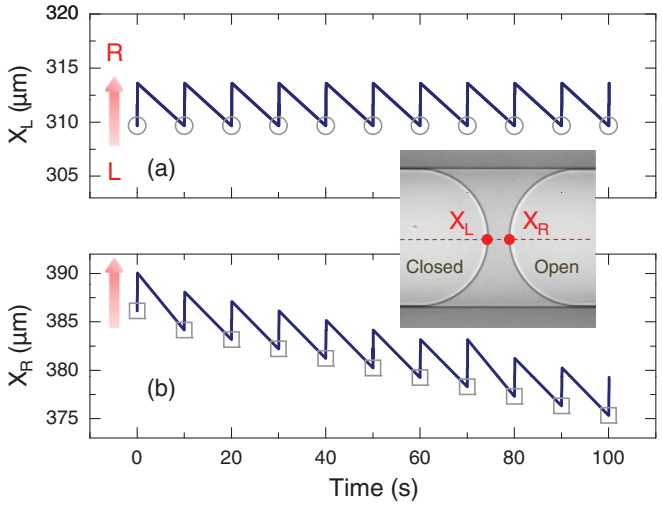

FIG. 3. (Color online) High reversibility of the x-ray-induced vaporization. The variances in the positions of the left [marked as X_L in (a)] and the right meniscus apexes [marked as X_R in (b)] were tracked for ten cycles for 100.1 s. The position changes during the short exposure of 100 ms and the pause of 9.9 s were very repeatable for every cycle. The rapid shifts of 3.9 μm for 100 ms in both X_L and X_R were induced by the x-ray irradiation (∼0.1 ph Å^{-2}). After the pause, the left meniscus was completely recovered, as can be clearly seen by the same positions of the circles, whereas the right one continued to decrease with time, as seen by the squares. The gradual decreases in X_R at a rate of 1.0 μm for 10 s were induced by natural vaporization. This result shows that the x-ray-induced switching is highly reversible in both of the menisci.

40% humidity. The evaporation rate for the open-open system was very high as ∼62 pL s^{-1} [=slope (2.8 × 10^{-4} s^{-1}) × initial volume (222 nL); open circles] by the convection effect [16], whereas the closed-closed system (closed circles) showed no evaporation. We find good agreement in the natural evaporation rates for the open-closed systems (Figs. 4 and 5), supporting

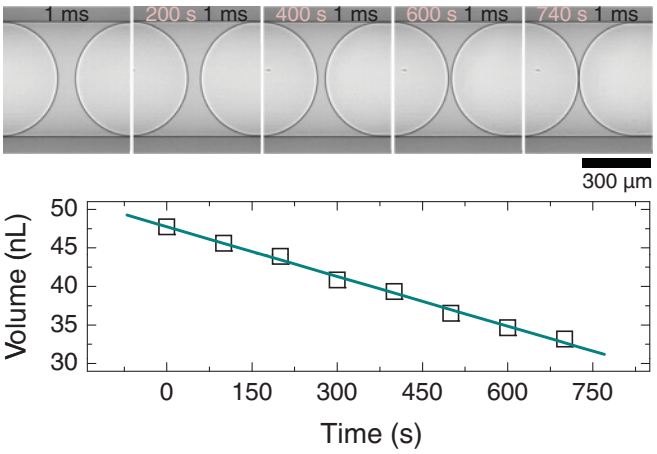

FIG. 4. (Color online) Natural vaporization rates with x-ray irradiation. X-ray snapshots of the water menisci showed gradual water shrinkage by natural vaporization only in the open (right) region but not in the closed (left) region. The natural vaporization rate measured from the water volume changes was 20 ± 0.6 pL s^{-1} for the total cycles of 740 s.

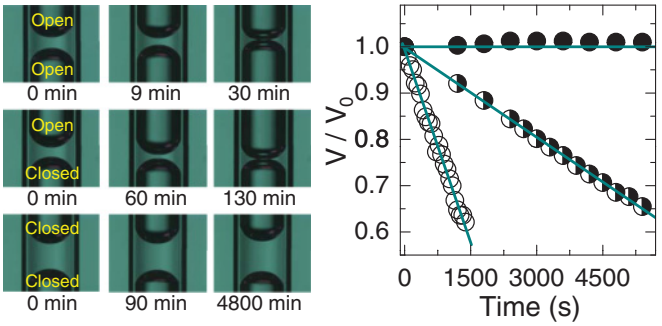

FIG. 5. (Color online) Natural vaporization rates without x-ray irradiation. Optical micrographs for monitoring water volume changes within open-open, open-closed, and closed-closed capillary systems ($2R$ = 800 μm) with time. The length of the open region was ∼10 mm for all systems. The evaporation rates were measured as ∼14 pL s^{-1} for the open-closed case (half-closed circles) and ∼62 pL s^{-1} for the open-open case (open circles). The closed-closed case (closed circles) showed no evaporation.

no influence of the x-ray irradiation on the natural evaporation rate.

Notably, x-ray-induced vaporization is quantitatively different from radiolysis-induced gas generation for water [17]. The x-ray-induced vapor expansion rate of ∼770 pL for ∼0.1 ph Å^{-2} (≈5 kGy) at 300 K, corresponding to ∼7 nmol MGy^{-1}, is much larger than the radiolysis-induced gas generation rate of ∼0.05 nmol MGy^{-1} at 5 K or ∼0.01 nmol MGy^{-1} at 100 K [17]. In addition, radiolysis-induced gas generation becomes negligible over 100 K and is obviously irreversible [17]. X-ray-induced vaporization is therefore irrelevant to radiolysis.

Is the closed air region warmed up *directly* by the x-ray irradiation? An ∼560 μm shift is expected by the thermal expansion, $\Delta V = \alpha P/C_p$, based on $\Delta V = \alpha V \Delta T$ and $\Delta T = P/(C_p \mathrm{V})$, where ΔT is the temperature rise, α is the thermal-expansion coefficient (3.50 × 10^{-3} K^{-1} [18]), C_p is the heat capacity (1.17 mJ cm^{-3} K^{-1} [19]), and P is the absorbed power passing through the closed air region. Here, $P \approx$ 25 μJ by multiplying the x-ray power (8 W mm^{-2}) by the irradiation time (0.1 s), the sample area (∼1/4 mm^2), and the absorption rate (∼0.012% for 500-μm-thick air at 13 keV [20]). The expected thermal shift (560 μm) is inconsistent with the actual shift (3.9 μm in Fig. 3). The expected heating, $\Delta T \approx$ 184 K for 0.1 s at 250 μJ s^{-1} for V = 115 nL, is unrealistic, because >99.9% of the total attenuation of the beam is used up for nonthermal photoelectric absorption [21] and gas heating can occur only by extremely high fluxes (e.g., 10^{37} J s^{-1} [22]). Indeed, x-ray heating was negligible in the previous measurements [7,23]. X-ray-induced vaporization is therefore not due to heating effect.

X-ray-induced vaporization is thus attributed to a photoionization-induced surface-tension reduction, which decreases the vaporization enthalpy, as previously hypothesized [7]. The reversibility of x-ray-induced vaporization (Fig. 3) can be explained by a reversible change of the enthalpy [10,11]. The charges accumulated from x-ray-induced ionization, which results in the surface-tension reduction, are relaxed

during the recess, allowing the surface tension to recover and thus reversibly inducing vapor condensation.

Our result suggests that photoionization induces vaporization by a significant surface-tension reduction. The surface tension [γ (mN m^{-1})] varies from the original value (γ_0) with the surface charge density [σ (C m^{-2})] below the Rayleigh limit ($\sigma_R \approx 6.89 \times 10^{-4}$ C m^{-2} for water) as $\gamma = \gamma_0 [1 + 4(\sigma/\sigma_R)^2]^{-1/2}$ [9]. The latent heat of vaporization [H (J g^{-1})] depends on the surface tension as $H \approx 581.1\ \gamma^{1/3}$ (estimated for water from [10] at 0.01−374.15 °C; the coefficient of determination is $R^2 = 0.999\,42$) and thus has a general relation with the photoionization as

$$H \approx 581.1\ \gamma_0^{1/3}[1 + 4(\sigma_R)^2]^{-1/6}.$$

Here the vapor flux (J) is inversely proportional to H at a fixed heat transfer ($Q = HJ$) [24], implying ∼20% increase in J by ionization of $\sigma \approx 0.8\sigma_R$, which is comparable to our result that the x-ray-induced vaporization rate (5.5 pL s^{-1}) is ∼28% of the natural rate (20 pL s^{-1}). This physical linkage has importance in radiological and electrohydrodynamic situations. This linkage may explain why bubbles within biological samples are generated and/or expanded by high-brilliance x-ray photons, which has been a critical problem in x-ray biological imaging [25]. Ionization-induced vaporization can be a significant source of vapor generation and may accelerate evaporation of charged drops in electrohydrodynamic situations such as electrification of aerosols, combustion of fuel droplets, spray painting, and inkjet printing [26,27].

To conclude, we provide quantitative evidence of x-ray-induced water vaporization in a closed capillary tube using high-speed phase-contrast x-ray imaging. This x-ray-induced effect can be fully recovered by a sufficient pause in the irradiation. High-brilliance x rays can modify material properties, including surface tension and viscosity [28]. A very short exposure on the μs time scale would be useful to prevent any x-ray-induced changes [29,30]. Finally, we stress that the x-ray irradiation barrier for vaporization (∼0.1 photons per Å^2) is much less than the conventional damage barrier (∼200 photons per Å^2) by the Coulomb explosion [2]. The new barrier is important in supporting sample stability and safety from radiation damage with high-brilliance x-ray sources. This result is of significance in carrying out x-ray experiments for high-resolution analysis of small confined water or living tissues. Ionization-induced vaporization will be universally important in electrohydrodynamics of charged drops and in biological imaging when using ionizing radiation sources besides x-ray sources.

ACKNOWLEDGMENTS

This research was supported by the Creative Research Initiatives (Functional X-ray Imaging) of MEST/NRF. Use of the Advanced Photon Source, an Office of Science User Facility operated for the US Department of Energy (DOE) Office of Science by Argonne National Laboratory, was supported by the US DOE under Contract No. DE-AC02-06CH11357.

[1] A. Sakdinawat and D. Attwood, Nature Photon. **4**, 840 (2010).
[2] R. Neutze *et al.*, Nature (London) **406**, 752 (2000).
[3] R. Henderson, Proc. R. Soc. London B **241**, 6 (1990).
[4] D. Duft *et al.*, Nature (London) **421**, 128 (2003).
[5] I. Last Y. Levy, and J. Jortner, Proc. Natl. Acad. Sci. USA **107**, 1094 (2010).
[6] T. D. Märk and P. Scheier, Nat. Phys. **6**, 82 (2010).
[7] B. M. Weon, J. H. Je, Y. Hwu, and G. Margaritondo, Phys. Rev. Lett. **100**, 217403 (2008).
[8] B. M. Weon, J. H. Je, Y. Hwu, and G. Margaritondo, Appl. Phys. Lett. **92**, 104101 (2008).
[9] B. M. Weon and J. H. Je, Appl. Phys. Lett. **93**, 244105 (2008); **96**, 194101 (2010).
[10] D. C. Agrawal and V. J. Menon, Phys. Rev. A **46**, 2166 (1992).
[11] J. Garai, Fluid Phase Equilib. **283**, 89 (2009).
[12] K. Fezzaa and Y. Wang, Phys. Rev. Lett. **100**, 104501 (2008).
[13] Y. Wang *et al.*, Nat. Phys. **4**, 305 (2008).
[14] H. Fujioka, S. Takayama, and J. B. Grotberg, Phys. Fluids **20**, 062104 (2008).
[15] See Supplemental Material at http://link.aps.org/supplemental/10.1103/PhysRevE.84.032601 for sequential x-ray micrographs for the first five cycles.
[16] H. Wang, J. Y. Murthy, and S. V. Garmella, Int. J. Heat Mass Transf. **51**, 3007 (2008).
[17] A. Meents, S. Gutmann, A. Wagner, and C. Schulze-Briese, Proc. Natl. Acad. Sci. USA **107**, 1094 (2010).
[18] J. A. Fay, *Introduction to Fluid Mechanics* (MIT Press, Cambridge, 1994).
[19] *CRC Handbook of Chemistry and Physics*, 74th ed., edited by D. R. Lide (CRC, Boca Raton, 1993).
[20] J. H. Hubbell and S. M. Seltzer, *Tables of X-Ray Mass Attenuation Coefficients and Mass Energy-Absorption Coefficients* (NIST, Gaithersburg, 1995).
[21] A. G. Peele *et al.*, Phys. Rev. A **66**, 042702 (2002).
[22] P. R. Maloney, D. J. Hollenbach, and A. G. G. M. Tielens, Astrophys. J. **466**, 561 (1996).
[23] J. J. Socha *et al.*, BMC Biology **5**, 6 (2007).
[24] L. Yu. Barash, T. P. Bigioni, V. M. Vinokur, and L. N. Shchur, Phys. Rev. E **79**, 046301 (2009).
[25] A. Momose *et al.*, Jpn. J. Appl. Phys. **45**, 5254 (2006).
[26] C. D. Stow, Rep. Prog. Phys. **32**, 1 (1969).
[27] R. M. Thaokar and S. D. Deshmukh, Phys. Fluids **22**, 034107 (2010).
[28] B. M. Weon *et al.*, Phys. Rev. Lett. **107**, 018301 (2011).
[29] B. M. Weon, J. H. Je, and C. Poulard, AIP Advances **1**, 012102 (2011).
[30] J. S. Lee *et al.*, Nature Commun. **2**, 367 (2011).